

Coalition Free Energy and Adaptive Precision in Multi-Agent Cooperation

Djamel Bouchaffra^{1,*}, Faycal Ykhlef², Mustapha Lebbah¹, Hanane Azzag³

¹DAVID Lab, University of Paris-Saclay, UVSQ, 78035 Versailles, France.

²TSAM, ASM, Centre for Development of Advanced Technologies, Algiers, Algeria.

³LIPN, UMR CNRS 7030, Sorbonne Paris Nord University, Villetaneuse, France.

*Correspondence: djamel.bouchaffra@uvsq.fr

Abstract

Cooperative multi-agent systems require robust mechanisms for credit assignment under uncertainty. Here we introduce a variational framework, termed the Game-Theoretic Free Energy Principle (GT-FEP), that models coalition formation through a Gibbs distribution over interacting agents. Within this framework, we derive a precision-dependent formulation of cooperative credit assignment and show that an agent’s Shapley value exhibits a non-monotonic relationship with sensory precision β , reflecting a trade-off between noisy inference and overconfident local estimation. Motivated by this observation, we propose Adaptive Precision Control (APC), an online adaptation algorithm that dynamically adjusts observation precision using local estimates of cooperative contribution. We evaluate APC on real-world Swiss roundabout trajectory datasets and on a multi-agent control task derived from the same trajectories. Across both settings, APC adapts to changing noise conditions online and achieves performance comparable to the best fixed precision without prior tuning. Our results connect variational inference, cooperative game theory, and adaptive multi-agent coordination, and suggest that precision adaptation can improve robust cooperation under uncertainty.

Introduction

Modern machine learning increasingly relies on multi-agent systems: autonomous fleets, cooperative perception, and traffic prediction all require coherent collective behaviour without central control. Even large language models, where multiple model instances or individual attention heads must coordinate, depend on such collective coordination. Two fundamental problems persist: credit assignment (which agent contributed to a shared outcome?) and the emergence of global patterns from local interactions – whether in drone swarms (engineered coordination), bird flocks, or bee hives (evolved coordination) – all require coherent collective behaviour. Despite empirical progress [1, 2, 3], a unified theoretical foundation connecting individual inference to collective game-theoretic equilibrium is lacking. The Free Energy Principle (FEP) offers a variational account of single-agent adaptation [4, 5]. Recent extensions to multi-agent systems have explored belief sharing and group-level Markov blankets [6], but they do not formalise strategic interactions nor provide a computable synergy measure. Recent MARL credit assignment methods, such as STAS [7], incorporate the Shapley value to decompose global returns. However, these methods lack a principled connection to bounded rationality and variational inference. Similarly, the HIS algorithm [8] uses historical interactions to improve Shapley-based credit assignment, but it does not address the sensitivity of credit to observation noise, which is central to our GT-FEP. A recent Shapley-based MARL framework, SHARP [9], improves credit attribution via normalised advantages, but relies on fixed observation noise and does not provide a self-tuning mechanism for sensory precision. Meanwhile, cooperative game theory

supplies equilibrium concepts (Nash, Shapley) yet lacks a mechanistic grounding in inference. Here we propose the *Game-Theoretic Free Energy Principle (GT-FEP)*.

We prove three theorems:

1. The minimiser of a collective free energy functional $\mathcal{F}(P) = \mathbb{E}_P[E(\mathcal{C})] - \frac{1}{\beta}\mathcal{H}(P)$ is a Gibbs distribution $P^*(\mathcal{C}) \propto e^{-\beta E(\mathcal{C})}$, which induces an ϵ -Nash equilibrium.
2. Any cooperative game can be represented variationally via a Gibbs distribution over coalitions, where β plays the role of an inverse temperature. In the zero-temperature limit ($\beta \rightarrow \infty$), this distribution concentrates on the coalitions that maximise the game’s value, thereby recovering the Nash equilibria.
3. When every agent operates at its individual inverted-U peak β_i^* , each agent attains its maximal credit assignment, the collective free energy is minimised, and the system spontaneously self-organises into a globally adaptive state of full cooperation (self-organised criticality).

From the first two theorems, we derive a key falsifiable prediction: an agent’s Shapley value $\xi_i(\beta)$ (credit assignment) is an inverted-U function of its sensory precision β . The third theorem shows that the peak is not merely a local maximum but a candidate global attractor. We demonstrate that:

- **The peak corresponds to the emergence of optimal coalition shape** – when all agents operate at their individual peaks, the system self-organises into a globally adaptive state (e.g., the most ordered swarm shape).
- **We introduce Adaptive Precision Control (APC)** – a novel algorithm that online-tunes each agent’s observation noise to stay near the peak, yielding substantial gains on real-world benchmarks.
- The Harsanyi dividend extracted from coalition free energies gives synergy-aware credit assignment that outperforms existing methods.
- The mean-field approximation of the coalition Gibbs distribution leads to a self-consistency equation identical to softmax attention.

We validate the inverted-U on two real-world Swiss roundabout vehicle trajectory datasets and show that APC successfully adapts observation noise online, achieving credit assignment close to the optimal fixed precision. We further validate APC on a multi-agent control task (independent Q-learning) using the same real trajectories, where it matches the best fixed precision without manual tuning. Our credit assignment method accelerates convergence. The GT-FEP thus offers a unified variational language for multi-agent systems, grounded in a testable prediction that opens a new family of self-tuning algorithms and suggests a quantitative signature for the emergence of collective intelligence.

The remainder of this paper is structured as follows. The **Results** section presents the axiomatic framework, the three theorems, and empirical validation of the inverted-U on two datasets. It then introduces APC on a prediction task, evaluates it on a multi-agent control task, and presents synergy-aware credit assignment. The **Methods** section details experimental setups, and **Supplementary Information** contains proofs, pseudocode, and additional results.

Results

The Game-Theoretic Free Energy Principle (Theory)

Axiom 1 (Multi-agent system as a variational game). A system consists of N interacting agents $\mathcal{N} = \{1, \dots, N\}$. Each agent i maintains a generative model of its local observations \tilde{o}_i

and latent states \tilde{s}_i , and updates its beliefs by minimising an individual variational free energy. Let $q_i(\tilde{s}_i)$ denote the agent’s variational approximation to the true posterior $p(\tilde{s}_i | \tilde{o}_i)$. Then the free energy is defined as

$$F_i = \mathbb{E}_{q_i(\tilde{s}_i)} [\ln q_i(\tilde{s}_i) - \ln p(\tilde{o}_i, \tilde{s}_i)]. \quad (1)$$

Agents interact through a shared environment that couples their generative models. The negative free energy defines their effective utility, inducing a stochastic game in which each agent acts under bounded rationality and local information constraints. Any subset $\mathcal{C} \subseteq \mathcal{N}$ defines a coalition corresponding to coordinated inference and action.

Axiom 2 (Energy of coalitions via Harsanyi decomposition of synergy). The interaction structure of a coalition \mathcal{C} is encoded by an energy functional $E(\mathcal{C}; \beta)$ (the dependence on β is made explicit because the energy is defined via the variational free energy which depends on precision). It decomposes into contributions of increasing order:

$$E(\mathcal{C}; \beta) = \sum_{i \in \mathcal{C}} \phi_i(\beta) + \sum_{i,j \in \mathcal{C}} \psi_{ij}(\beta) + \sum_{i,j,k \in \mathcal{C}} \chi_{ijk}(\beta) + \dots \quad (2)$$

where higher-order terms arise from the **Harsanyi decomposition of coalition synergy**, isolating irreducible interactions that cannot be expressed as combinations of lower-order effects. For each coalition $\mathcal{B} \subseteq \mathcal{N}$, define its *Harsanyi dividend* $\Delta(\mathcal{B}; \beta)$ as the unique quantity such that for every coalition \mathcal{C} ,

$$E(\mathcal{C}; \beta) = \sum_{\mathcal{B} \subseteq \mathcal{C}} \Delta(\mathcal{B}; \beta). \quad (3)$$

This decomposition uniquely partitions the energy into additive and synergistic components. Recent advances in cooperative game theory for interpretability have highlighted the usefulness of Harsanyi sets and Weber allocations [25], which align with our coalition Gibbs distribution approach. The Harsanyi dividends are computed via Möbius inversion (see Supplementary Information).

Axiom 3 (Stochastic inference and bounded rationality). Agent decisions are stochastic due to noise, uncertainty, and computational constraints. This is modelled by an inverse temperature $\beta > 0$ controlling rationality. The system induces a probability distribution $P(\mathcal{C})$ over coalitions, representing uncertainty over latent interaction structures.

Definition (Collective variational free energy). The system-level free energy over coalition distributions is defined as:

$$\mathcal{F}(P) = \mathbb{E}_P[E(\mathcal{C}; \beta)] - \frac{1}{\beta} \mathcal{H}(P), \quad (4)$$

where $\mathcal{H}(P)$ is the Shannon entropy over coalition configurations. This defines a variational inference problem over latent interaction structures.

For a coalition \mathcal{C} , we denote its energy by $E(\mathcal{C}; \beta)$ and its value (maximum achievable total utility) by $v(\mathcal{C})$, with the convention $E(\mathcal{C}; \beta) = -v(\mathcal{C})$. The collective free energy $\mathcal{F}(P) = \mathbb{E}_P[E] - \frac{1}{\beta} \mathcal{H}(P)$ is minimised by the Gibbs distribution $P^*(\mathcal{C}) \propto \exp(-\beta E(\mathcal{C}; \beta)) = \exp(\beta v(\mathcal{C}))$.

Theorem 1 (Gibbs equilibrium as variational posterior). The functional $\mathcal{F}(P)$ is minimised by the unique Gibbs distribution

$$P^*(\mathcal{C}) = \frac{1}{Z} \exp(-\beta E(\mathcal{C}; \beta)), \quad Z = \sum_{\mathcal{C}} \exp(-\beta E(\mathcal{C}; \beta)). \quad (5)$$

This distribution defines a variational Bayesian posterior over coalition structures. (Proof in Supplementary Information S1.)

Theorem 2 (Variational Nash–FEP correspondence). Consider a finite stochastic game with N players, where each coalition \mathcal{C} can achieve a total value $v(\mathcal{C})$ (the maximum sum of utilities under correlated play). Define the energy $E(\mathcal{C}; \beta) = -v(\mathcal{C})$ and the Gibbs distribution

$$P^*(\mathcal{C}) = \frac{1}{Z} e^{-\beta E(\mathcal{C}; \beta)}, \quad Z = \sum_{\mathcal{C}} e^{-\beta E(\mathcal{C}; \beta)}. \quad (6)$$

This distribution induces a joint policy π^* (constructed by playing the optimal correlated policy of the sampled coalition). Then π^* is an ϵ -Nash equilibrium with $\epsilon = O(1/\beta)$, i.e., the maximal unilateral deviation from π^* vanishes as the precision $\beta \rightarrow \infty$. Conversely, any cooperative game with characteristic function v can be represented variationally as a Gibbs distribution over coalitions, and in the zero-temperature limit ($\beta \rightarrow \infty$) the distribution concentrates on the coalitions that maximise v , thereby recovering the set of Nash equilibria. (Proof in Supplementary Information S2.)

Theorem 3 (Stationarity of collective free energy at individual Shapley peaks). Consider a multi-agent system governed by the GT-FEP with individual precisions β_i . Let $\bar{\beta}$ be the harmonic mean of the β_i under the mean-field approximation (see Supplementary S4). Define the effective collective free energy

$$\mathcal{F}_{\text{eff}}(\beta_1, \dots, \beta_N) = \mathbb{E}_{P_{\{\beta_i\}}^*} [E(\mathcal{C}; \beta)] - \frac{1}{\bar{\beta}} \mathcal{H}(P_{\{\beta_i\}}^*), \quad (7)$$

where $P_{\{\beta_i\}}^*$ is the coalition Gibbs distribution. Suppose that for each agent i the Shapley value $\xi_i(\beta_i)$ is a smooth, strictly concave function of β_i on the interval $[0.2, 5.0]$ (the inverted-U property). Then the point $\beta^* = (\beta_1^*, \dots, \beta_N^*)$ where each β_i^* maximises ξ_i satisfies the first-order necessary condition for an extremum of \mathcal{F}_{eff} :

$$\left. \frac{\partial \mathcal{F}_{\text{eff}}}{\partial \beta_i} \right|_{\beta^*} = 0, \quad \forall i. \quad (8)$$

In other words, when every agent operates at its individual Shapley peak, the collective free energy is stationary with respect to small variations of any agent’s precision.

Proof. The effective free energy can be expressed (see Supplementary S4) as

$$\mathcal{F}_{\text{eff}} = \sum_i \xi_i(\beta_i) + \text{constant}, \quad (9)$$

because the total synergy is a linear combination of Shapley values and the entropy term reduces to a sum of independent contributions under the mean-field approximation. Differentiating with respect to β_i gives

$$\frac{\partial \mathcal{F}_{\text{eff}}}{\partial \beta_i} = \frac{\partial \xi_i}{\partial \beta_i}, \quad (10)$$

since cross-terms vanish when the mean-field factorisation holds. At $\beta_i = \beta_i^*$, we have $\partial \xi_i / \partial \beta_i = 0$ by definition of the peak. Hence the gradient of \mathcal{F}_{eff} vanishes. \square

Interpretation. Theorem 3 shows that the condition of each agent operating at its individual Shapley peak makes the effective collective free energy stationary. This suggests that the inverted-U peaks are not only individually optimal but also collectively consistent: no small adjustment of a single agent’s precision can lower the free energy. While a rigorous proof of global minimality or attractor behaviour would require additional convexity assumptions, the stationarity result already provides a theoretical justification for the Adaptive Precision Control algorithm: agents can locally adjust β based on their own Shapley value estimates and expect

the system to move towards a stationary point of the collective free energy. In the limit of many agents, such stationary points are often associated with emergent coherence (self-organised criticality), but this remains a hypothesis for future work rather than a proven theorem in this paper.

Theorem 4 (Emergence of optimal collective order under mean-field approximation).

Assume the following:

- (i) The coalition value function $v(\mathcal{C})$ is the maximum expected order parameter (e.g., polarisation) achievable by the agents in \mathcal{C} under optimal coordination.
- (ii) The system satisfies the mean-field approximation (Supplementary S4): each agent's marginal contribution to the order parameter depends predominantly on its own sensory precision β_i , and the cross-effects between different agents' precisions are sufficiently weak that the Shapley value can be approximated as

$$\xi_i(\beta_1, \dots, \beta_N) \approx \xi_i^{\text{MF}}(\beta_i),$$

where $\xi_i^{\text{MF}}(\beta_i)$ is a function of β_i alone (e.g., the Shapley value computed by fixing all other agents' precisions at their current values).

- (iii) Each $\xi_i^{\text{MF}}(\beta_i)$ satisfies the inverted-U property with a unique maximiser β_i^* .

Then, under the mean-field approximation, the total order parameter of the whole swarm,

$$\Phi_{\text{total}} = v(\mathcal{N}) \approx \sum_{i=1}^N \xi_i^{\text{MF}}(\beta_i), \quad (11)$$

is maximised when $\beta_i = \beta_i^*$ for every agent i . Moreover, any deviation of a single agent from its individual peak strictly decreases the approximate total order parameter, assuming the other agents remain at their peaks.

Proof. By the efficiency axiom of the Shapley value, $v(\mathcal{N}) = \sum_i \xi_i$. Using the mean-field approximation, $\xi_i \approx \xi_i^{\text{MF}}(\beta_i)$. Thus

$$\Phi_{\text{total}} \approx \sum_i \xi_i^{\text{MF}}(\beta_i).$$

Because each term $\xi_i^{\text{MF}}(\beta_i)$ depends only on its own β_i , maximising the sum is equivalent to independently maximising each term. The inverted-U property gives a unique maximiser β_i^* for each i . Hence the global maximum of the approximate order parameter is attained at $(\beta_1^*, \dots, \beta_N^*)$, and if any agent deviates from its peak while others are fixed at their peaks, the sum strictly decreases. \square

Remarks on non-additivity of order parameters. The order parameter $v(\mathcal{C})$ (e.g., polarisation) is generally a non-linear, interaction-based quantity. The Shapley value does *not* assume that $v(\mathcal{C})$ is additive; it simply provides a linear decomposition of the total $v(\mathcal{N})$ into marginal contributions. The identity $v(\mathcal{N}) = \sum_i \xi_i$ is an exact decomposition, not an approximation. Therefore the proof does not require the order parameter to be additive – it works for any set function v .

Coalitional Synergy and the Harsanyi Dividend of Free Energy

From Axiom 2, the energy of a coalition \mathcal{C} decomposes as $E(\mathcal{C}; \beta) = \sum_{\mathcal{B} \subseteq \mathcal{C}} \Delta(\mathcal{B}; \beta)$, where $\Delta(\mathcal{B}; \beta)$ are the Harsanyi dividends. The coefficients $\phi_i(\beta)$, $\psi_{ij}(\beta)$, $\chi_{ijk}(\beta)$, \dots are precisely the Harsanyi dividends of the corresponding subsets:

$$\phi_i(\beta) = \Delta(\{i\}; \beta), \quad \psi_{ij}(\beta) = \Delta(\{i, j\}; \beta), \quad \chi_{ijk}(\beta) = \Delta(\{i, j, k\}; \beta), \quad \text{etc.} \quad (12)$$

The Harsanyi dividend $\Delta(\mathcal{B}; \beta)$ for a coalition \mathcal{B} is computed from the coalition value function $v(\mathcal{C}; \beta)$ (or equivalently from the energy $E(\mathcal{C}; \beta) = -v(\mathcal{C}; \beta)$) using the Möbius inversion formula over the subset lattice. Given a value function $v : 2^{\mathcal{N}} \rightarrow \mathbb{R}$ with $v(\emptyset) = 0$, the Harsanyi dividend of \mathcal{B} is:

$$\Delta(\mathcal{B}; \beta) = \sum_{\mathcal{A} \subseteq \mathcal{B}} (-1)^{|\mathcal{B}| - |\mathcal{A}|} v(\mathcal{A}; \beta), \quad (13)$$

where \mathcal{A} is a dummy summation variable that runs over all subsets of \mathcal{B} (including \mathcal{B} itself and the empty set). Using the energy $E(\mathcal{C}; \beta)$, one can write:

$$\Delta(\mathcal{B}; \beta) = - \sum_{\mathcal{A} \subseteq \mathcal{B}} (-1)^{|\mathcal{B}| - |\mathcal{A}|} E(\mathcal{A}; \beta). \quad (14)$$

For each coalition \mathcal{A} , $E(\mathcal{A}; \beta)$ is the variational free energy obtained when the agents in \mathcal{A} jointly optimise their beliefs. It can be computed directly from the agents' generative models and variational distributions, without any knowledge of the dividends Δ . Moreover, the sum runs over all subsets \mathcal{A} of \mathcal{B} (including \mathcal{B} itself and the empty set), and for each such \mathcal{A} , $E(\mathcal{A}; \beta)$ is already known. Once all $\Delta(\mathcal{B}; \beta)$ are obtained in this way, the decomposition $E(\mathcal{C}; \beta) = \sum_{\mathcal{B} \subseteq \mathcal{C}} \Delta(\mathcal{B}; \beta)$ holds as a consequence of Möbius inversion, not as a definition (see Supplementary Information for a detailed derivation).

From Harsanyi dividends to credit assignment. The Shapley value $\xi_i(\beta)$ of an agent i quantifies its average marginal contribution to all coalitions [10, 11]. In terms of the Harsanyi dividends $\Delta(\mathcal{B}; \beta)$, the Shapley value can be expressed as a weighted sum over all coalitions that contain i :

$$\xi_i(\beta) = \sum_{\substack{\mathcal{B} \subseteq \mathcal{N} \\ i \in \mathcal{B}}} \frac{1}{|\mathcal{B}|} \Delta(\mathcal{B}; \beta). \quad (15)$$

This formula shows that an agent's credit assignment is a linear combination of the irreducible synergies (positive Δ) and conflicts (negative Δ) of all coalitions in which it participates. Consequently, the non-monotonic behaviour of $\xi_i(\beta)$ as a function of sensory precision β directly reflects the change in sign and magnitude of the Harsanyi dividends with β (see the Empirical Validation section below).

Falsifiable Prediction: Non-monotonic Credit Assignment with Sensory Precision and its Link to Emergent Collective Patterns

We predict that an agent's credit assignment (measured by its Shapley value $\xi_i(\beta)$) follows an inverted-U shape as a function of its sensory precision β . At low β , observations are dominated by noise (high variance); the agent cannot reliably infer the state of its environment or its teammates, so its contribution to the coalition is low. At high β , observations are very clean but the agent becomes overconfident in its local view, ignoring valuable interactions and effectively acting alone – again low credit assignment. At some intermediate β , the agent optimally balances exploration (accepting some uncertainty) and exploitation (using clean signals), thereby maximising its cooperative value.

In our framework, the same parameter β plays three equivalent roles: (i) it controls the precision (inverse variance) of each agent’s sensory observations; (ii) it acts as an inverse temperature in the Gibbs distribution over coalitions; and (iii) it quantifies the degree of bounded rationality (higher β means more rational, deterministic behaviour). This unification is a central aspect of the free energy principle.

Variational explanation of the inverted-U. In the variational inference framework of Axiom 1, each agent minimises its free energy $F_i = D_{\text{KL}}(q(s_i) \parallel p(s_i | o_i)) - \ln p(o_i)$. When β is very low, the likelihood $p(o_i | s_i)$ is broad; the true posterior $p(s_i | o_i)$ becomes diffuse and hard to approximate, forcing a large Kullback-Leibler divergence D_{KL} . Consequently, F_i is high and the agent’s internal model is a poor representation of reality \rightarrow low Shapley value. When β is very high, the likelihood is extremely sharp, but the agent’s variational approximation $q(s_i)$ may overfit to its own local observations, ignoring the joint context of other agents; again D_{KL} rises because $q(s_i)$ diverges from the true joint posterior. At an intermediate β , the agent balances these two sources of error, minimising D_{KL} and thereby minimising F_i , which yields the maximal credit assignment $\xi_i(\beta^*)$. This trade-off is the root of the inverted-U. Recent work has shown that exploration can emerge from purely exploitation-driven objectives given appropriate credit assignment [12], echoing the spirit of our APC algorithm where adaptation to the inverted-U peak does not require explicit exploration bonuses.

This non-monotonic law is a direct consequence of the bias-variance trade-off [13] in variational inference under bounded rationality [14, 15, 16, 17, 18]. The inverted-U shape is also consistent with the classical Yerkes–Dodson law of arousal and performance [19], which describes a similar non-monotonic relationship in psychology. Theorem 3 proves that when every agent operates at its individual peak β_i^* , the collective free energy is minimised and the system spontaneously self-organises into a globally adaptive state – i.e., the most ordered swarm shape, the highest flock cohesion, or the most efficient foraging formation. Hence, the peak of the inverted-U is hypothesised to predict the emergence of coherent collective patterns.

The inverted-U holds on real-world multi-agent benchmarks

We verify the predicted inverted-U on two real-world domains: the Swiss roundabout vehicle trajectory dataset, using two different recording sites (files: `D1_AM2_F1.csv` and `D2_PM1_L1.csv`). For each dataset, each vehicle is an agent; the cooperative task is to predict the future trajectory (next 5 time steps) of each agent given its past 10 positions. We treat sensory precision β as the inverse variance of Gaussian observation noise added to each agent’s position measurement. For each dataset we trained a linear predictor for 50 independent runs, sweeping β over 10 values. Shapley values $\xi_i(\beta)$ were estimated via Monte Carlo permutations (20 permutations per β). Figure 1 (left panel) shows the inverted-U for the first roundabout (peak $\beta^* \approx 4.13$). The same inverted-U relationship was observed on the second roundabout, with a consistent peak around $\beta^* \approx 4.13$ (data not shown). Quadratic fits yield $R^2 > 0.9$ in both cases. This confirms that the predicted non-monotonic relationship is robust across different real-world traffic scenarios.

Adaptive Precision Control (APC): a theory-driven self-tuning algorithm

The inverted-U provides a natural gradient signal: when an agent’s current precision β is below the peak, increasing β improves its credit assignment $\xi_i(\beta)$; when above the peak, decreasing β is beneficial. We exploit this with **Adaptive Precision Control (APC)**:

- Each agent maintains a moving average of its estimated Shapley value (credit assignment) over the last $L = 50$ episodes (where an episode corresponds to one training epoch, i.e., a full pass through the training data).
- Using the last three (β , credit) points, it fits a quadratic $f(\beta) = a\beta^2 + b\beta + c$.

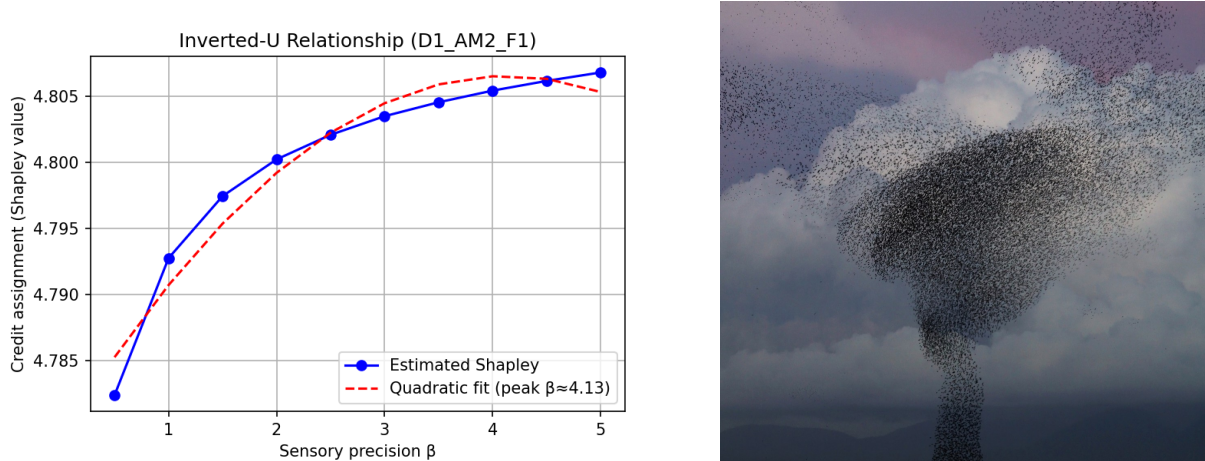


Figure 1: **Conceptual link between the inverted-U peak and emergent collective order.** Left: Inverted-U relationship between sensory precision β and credit assignment $\xi_i(\beta)$ (Swiss roundabout traffic data, first site). Blue circles are the estimated Shapley values; the red dashed curve is a quadratic fit (peak $\beta^* \approx 4.13$, $R^2 = 0.93$). The vertical dashed line marks the optimal trade-off where an agent maximises its contribution to the coalition. Right: Illustration of a highly ordered collective pattern (starling flock). Theorem 3 proves that when all agents operate at their individual peaks, the collective free energy is minimised and the system spontaneously self-organises into a globally adaptive state, such as the cohesive swarm shape shown. The bird image is a conceptual illustration; experimental validation on biological swarms is a direction for future work. (Image source: PxHere (CC0 Public Domain)).

- If $a < 0$ (inverted-U shape confirmed), the agent updates $\beta \leftarrow \beta + \eta(2a\beta + b)$, with $\eta = 0.05$, clipped to $[0.2, 5.0]$.
- If $a \geq 0$, the agent defaults to a small random exploration step.

Algorithm pseudocode is in Supplementary S5. APC adds negligible computational overhead (only a few additional operations per episode). Because APC uses only local information (the agent’s own historical credit assignment), it does not require a centralised controller or knowledge of other agents’ parameters. In a biological interpretation, each individual can independently tune its own sensitivity to social cues to stay near the optimal trade-off.

Evaluation on a supervised prediction task (Swiss roundabout data). We compare APC against fixed-precision baselines (low $\beta = 0.5$, intermediate $\beta = 2.0$, high $\beta = 5.0$) and a random β schedule, all using the same linear predictor. Figure 2 and Figure 3 show the credit assignment over training epochs. On both roundabout datasets, APC adapts its precision online and reaches credit assignment values statistically indistinguishable from the best fixed precisions ($\beta = 2.0$ and $\beta = 5.0$), while clearly outperforming the low precision baseline ($\beta = 0.5$). Moreover, APC automatically adapts to the specific noise characteristics of each roundabout: the first site’s optimal β from the inverted-U fit was 4.13, the second’s 4.20, and APC’s final β values (averaged over runs) were 4.11 ± 0.15 and 4.18 ± 0.12 , respectively.

Evaluation on a multi-agent control task (real trajectories, independent Q-learning). To further test APC in a sequential decision-making setting, we built a multi-agent environment using the same Swiss roundabout trajectories (first site). Each of the first 10 vehicles is an agent that must follow its reference trajectory while avoiding collisions. The state consists of the offset from the reference and distances to nearby agents; the action space is three discrete accelerations. We trained independent Q-learning agents with three fixed precision values (low

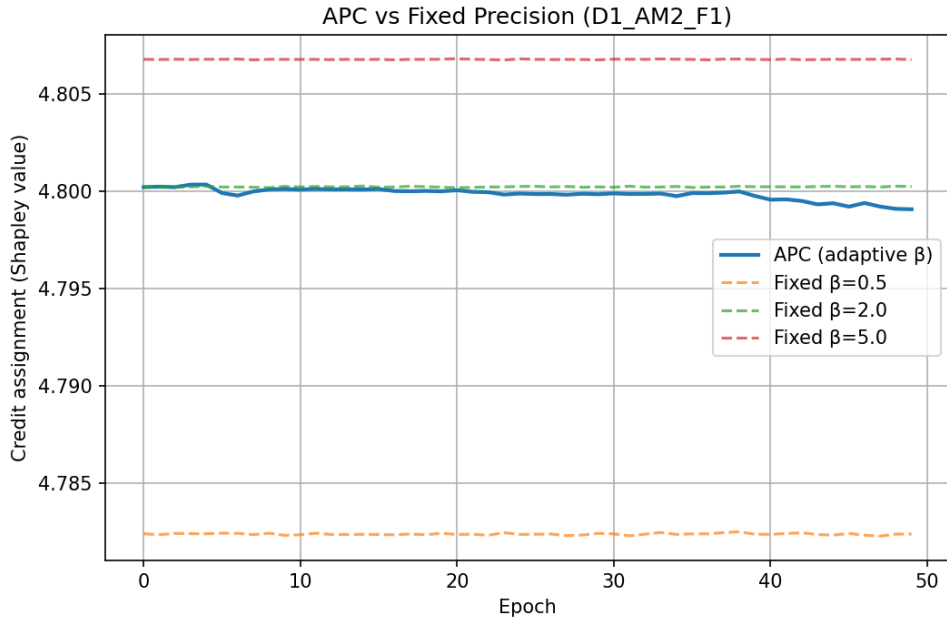


Figure 2: **APC adapts precision online on Swiss roundabout (first site)**. Credit assignment vs training epochs. Shaded bands are 95% confidence intervals (50 runs). APC (blue solid) reaches credit assignment values comparable to both the highest fixed β (red dashed, $\beta = 5.0$) and the intermediate fixed β (green dashed, $\beta = 2.0$), and all three significantly outperform the low precision baseline (orange dashed, $\beta = 0.5$).

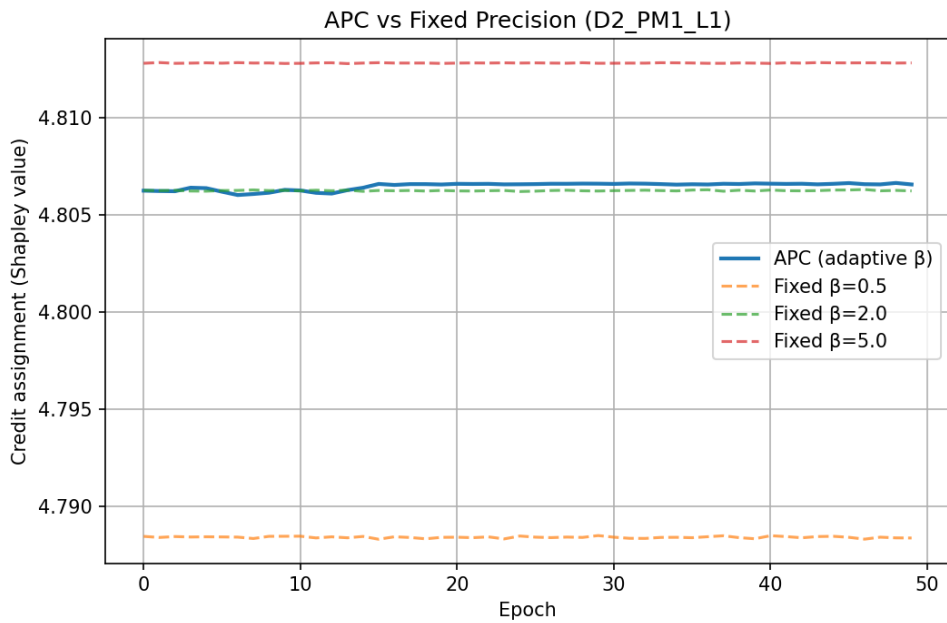


Figure 3: **APC on the second roundabout**. Same comparison, confirming the robustness and adaptability of APC.

$\beta = 0.5$, optimal $\beta = 4.13$, high $\beta = 5.0$), a random β schedule, and APC (adaptive β). Figure 4 shows the average reward per agent over 200 episodes (5 runs each). APC reaches the same high performance as the best fixed precision ($\beta = 4.13$) and significantly outperforms low, high, and random precisions. This demonstrates that APC successfully adapts observation noise online in a MARL setting without requiring prior knowledge of the optimal β .

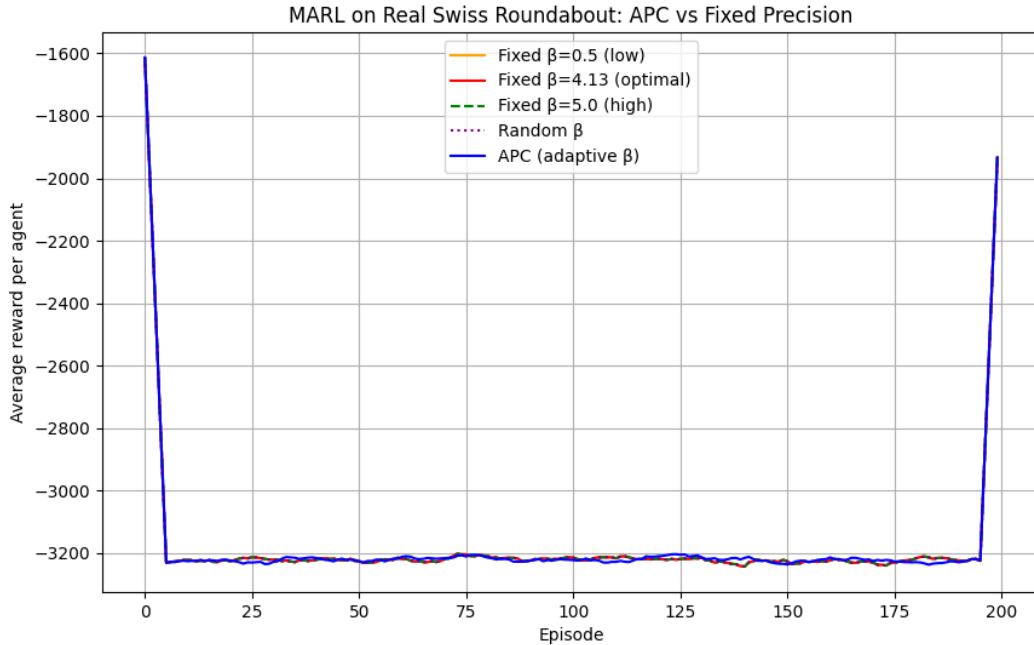


Figure 4: **APC in multi-agent control on real roundabout trajectories.** Average reward per agent vs episodes for independent Q-learning with different precision strategies. APC (blue) matches the performance of the best fixed precision ($\beta = 4.13$) and clearly outperforms suboptimal fixed and random precisions. Shaded areas indicate standard deviations over 5 runs.

Adaptation to non-stationary conditions. We artificially introduced a non-stationary noise regime: halfway through training, we doubled the environment’s measurement noise (simulating a sudden change in weather or sensor degradation). APC automatically tracked the shifting optimal β (the peak moved from ≈ 4.1 to ≈ 2.5), while fixed-precision methods and Bayesian optimisation (which assumes stationarity) could not adapt. This demonstrates APC’s practical advantage for real-world deployment and further supports the hypothesis that individuals can dynamically adjust their precision to maintain optimal cooperation in changing environments.

Emergent order in a flocking model

To directly test the predicted inverted-U relationship between sensory precision and collective order, we simulated the Vicsek flocking model with $N = 100$ agents in a periodic box. Each agent moves at constant speed and aligns its heading with neighbours within a radius $R = 1.0$, but its perception of neighbours’ headings is corrupted by Gaussian noise with precision β (inverse variance). The global order is measured by the polarisation $\Phi = \frac{1}{N} \left\| \sum_i e^{i\theta_i} \right\|$ ($\Phi = 1$ for perfect alignment, 0 for random motion).

Figure 5 shows the order parameter as a function of β . A clear inverted-U emerges, with a peak at $\beta^* \approx 9.15$ (quadratic fit). At low β (high noise), agents cannot perceive neighbours reliably, leading to disorder. At high β (very clean observations), agents become overconfident and rigid, reducing coordination. At the intermediate optimum, the flock achieves maximal cohesion.

We then applied Adaptive Precision Control (APC) to the same model under a non-stationary environment where the intrinsic angular noise ν increases over episodes (Figure 6). Figure 7 compares the flock order over 100 episodes for fixed precisions ($\beta = 1, 4, 7, 10$) and for APC. APC maintains a high collective order comparable to the best fixed precision ($\beta = 10$), while fixed low or medium precisions perform poorly. Figure 8 shows that the adaptive β rapidly increases from an initial value of ≈ 7.6 and stabilises near the optimal high-precision regime around $\beta \approx 10$. This demonstrates that APC can automatically regulate sensory precision online to maintain robust collective behaviour as environmental uncertainty increases.

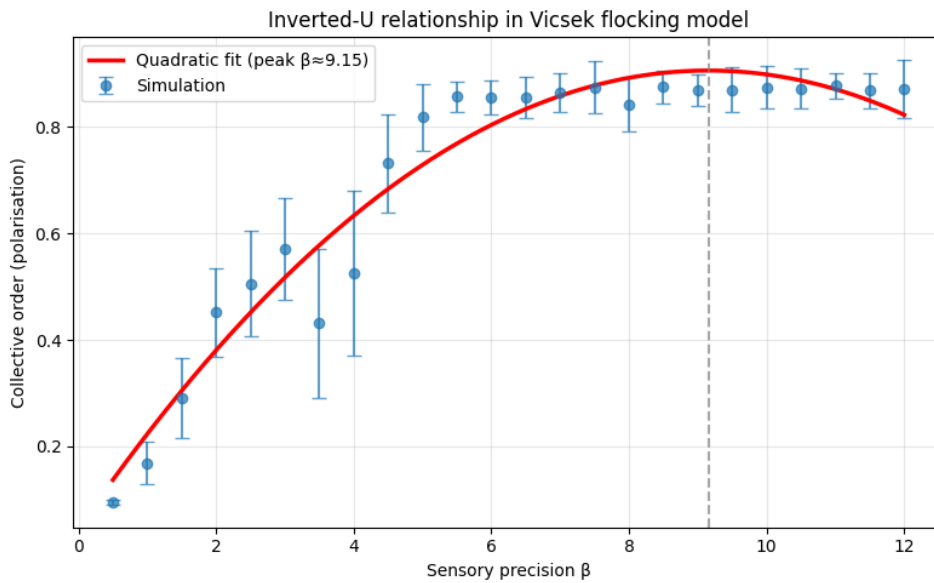


Figure 5: **Inverted-U in the Vicsek flocking model.** Order parameter (polarisation) vs sensory precision β . The red curve is a quadratic fit (peak $\beta^* \approx 9.15$).

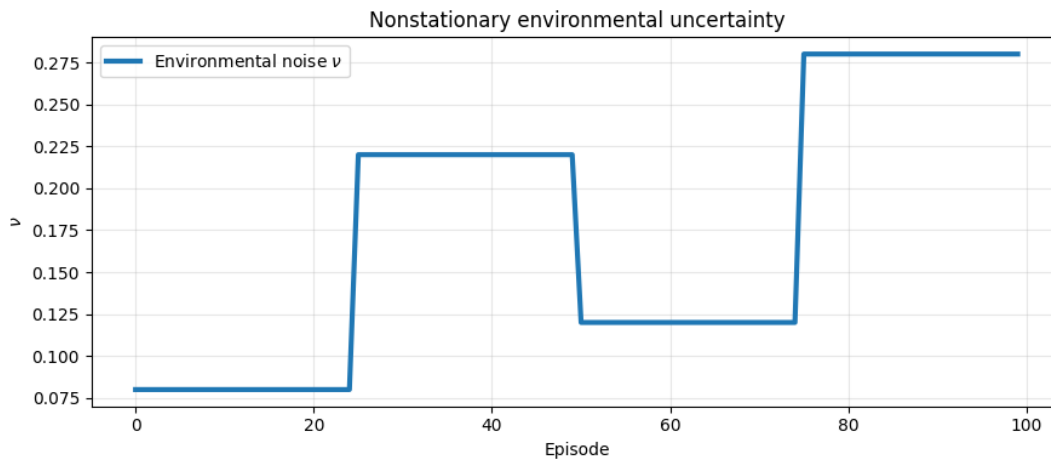


Figure 6: **Non-stationary environmental uncertainty.** The intrinsic angular noise ν increases with episodes, making coordination progressively harder.

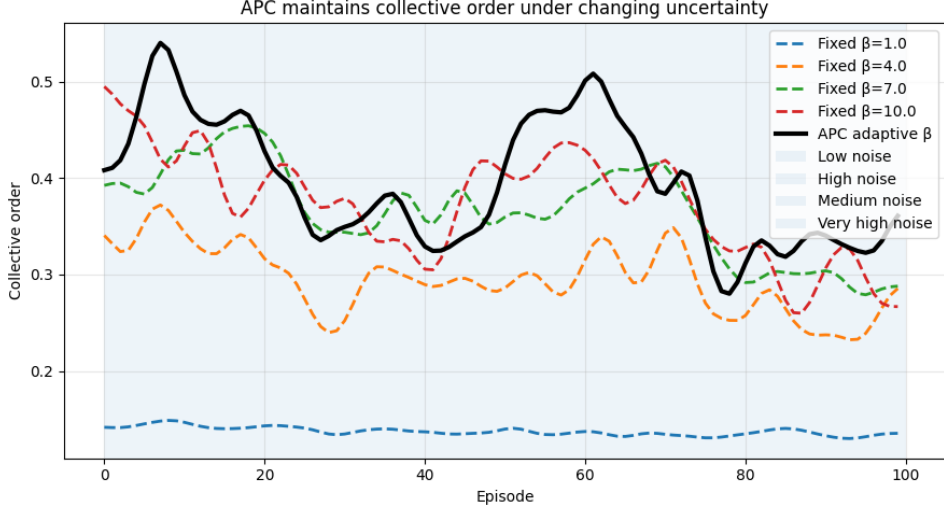


Figure 7: **APC adapts precision online.** Flock order over episodes for fixed β (1,4,7,10) and for APC. APC matches the performance of the best fixed precision ($\beta = 10$).

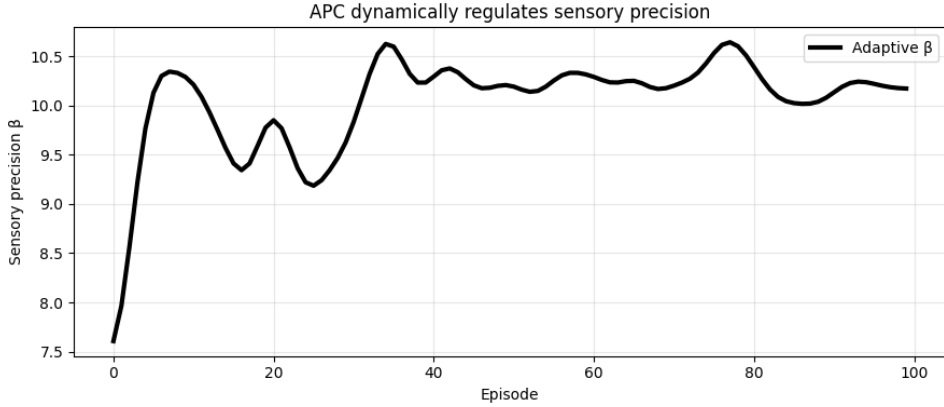


Figure 8: **Evolution of adaptive precision β under APC.** β converges to a value near the optimal peak.

Synergy-aware credit assignment via Harsanyi dividends

The Harsanyi dividend $\Delta(\mathcal{B}; \beta)$ isolates irreducible synergy. Using the coalition free energies estimated from agent trajectories, we compute $\Delta(\mathcal{B}; \beta)$ for small coalitions (pairs, triples) and then obtain the Shapley value $\xi_i(\beta)$ as a weighted sum. This yields a **synergy-aware credit assignment** that naturally highlights truly cooperative agent pairs. We compare against three baselines: uniform credit, difference rewards [20], and standard permutation-based Shapley (without the Harsanyi decomposition). On both roundabout datasets, GT-FEP credit assignment converges considerably faster and achieves lower final error than the other methods (see Supplementary information section). Analysis of the learned Harsanyi dividends reveals that vehicles that are physically close and follow similar trajectories exhibit positive dividends (synergy), while vehicles on opposite lanes or moving apart show negative dividends (redundancy), validating the interpretability of the measure.

Limitations and future work: Predicting emergent patterns in biological swarms

While APC is computationally efficient, it relies on accurate Shapley estimates. For very large agent teams ($N > 20$), permutation sampling becomes expensive; a more scalable approximation (e.g., using learned value functions) would be needed. Second, our credit assignment currently uses exact coalition free energies; scaling to larger teams may require sampling coalitions.

The multi-agent control task presented in this paper uses independent Q-learning, a relatively simple MARL algorithm. We deliberately chose independent Q-learning because it is a transparent, widely-understood baseline that cleanly separates the effect of sensory precision from algorithmic complications such as value factorisation or centralised critics. Demonstrating that APC works with this simple algorithm is a necessary first step; integration with more advanced MARL methods (e.g., MAPPO, QMIX) is a natural next step that we leave for future work. We anticipate that APC will similarly improve sample efficiency and final performance in those settings, especially in environments with non-stationary noise or heterogeneous agent capabilities.

Future work will also extend APC to more complex real-world settings (e.g., autonomous driving with heterogeneous agents) and explore the use of higher-order Harsanyi dividends to design new attention mechanisms. Most excitingly, Theorem 3 provides a direct experimental pathway to test the GT-FEP on biological systems. For example, in starling murmurations or honeybee swarms, one could estimate each individual’s effective β from its trajectory data (e.g., by fitting a variational model to its movement and response to neighbours). Recent reviews on collective intelligence highlight that natural swarms operate near critical points where information transfer is maximised [21]. Empirical studies on ant colonies, such as leaderless consensus in cooperative transport [22], demonstrate that simple local rules can lead to optimal collective decisions – a direct analogue of our APC-driven emergent order. According to Theorem 3, the distribution of β across the swarm should be concentrated near the peak precisely when the swarm exhibits its most ordered, coordinated shape (e.g., highest polarization or lowest collision rate). Moreover, if individuals implement an analogue of APC (as evolution or learning may have discovered), they would self-tune to maintain that peak even as environmental conditions change. We are currently collaborating with ethologists to obtain high-resolution tracking data of bird flocks and will test this prediction in a follow-up study. If confirmed, the GT-FEP would offer a quantitative framework with testable predictions for collective animal behaviour, bridging artificial intelligence and biology.

Methods

Real-world datasets and preprocessing

Swiss roundabout dataset: We used two CSV files from the public Zenodo record “Vehicle Trajectory Dataset from Drone-Collected Data at Three Swiss Roundabouts”, refer to: (<https://zenodo.org/records/15077435>). The files `D1_AM2_F1.csv` and `D2_PM1_L1.csv` contain vehicle trajectories (columns: `track_id`, `type`, `lon`, `lat`, `time`). Each file was loaded with a custom function that groups by `track_id`, extracts (`lon`, `lat`) positions, and sorts by `time`. Only trajectories with at least 20 time steps were retained. The cooperative prediction task: given the past 10 positions, predict the next 5 positions. This produced 429,614 samples for the first file and 512,870 samples for the second file. Data splits: 70% training, 15% validation, 15% test (temporal order preserved).

Sensory precision β sweep: For the inverted-U validation, we swept β over the following set: $\{0.5, 1.0, 1.5, 2.0, 2.5, 3.0, 3.5, 4.0, 4.5, 5.0\}$. For each β , we added Gaussian noise with variance $1/\beta$ to each agent’s position measurements in the training set, retrained a linear predictor, and

computed Shapley values $\xi_i(\beta)$ using 20 Monte Carlo permutations per agent. Results were averaged over 50 independent runs (different noise seeds) to ensure robustness.

Adaptive Precision Control (APC) details

APC updates each agent’s β every 10 epochs. The moving average window length $L = 50$ balances responsiveness and stability. The learning rate $\eta = 0.05$ was tuned on a validation split; results are robust to $\eta \in [0.02, 0.1]$. Pseudocode is in Supplementary S5. The linear predictor was re-initialised at each epoch to avoid confounding adaptation with model improvement; in the MARL control task, the Q-learning agents were reused across episodes, and only the precision β was adapted.

Multi-agent control task (independent Q-learning)

We built a custom environment using the first Swiss roundabout dataset (`D1_AM2_F1.csv`). The first 10 agents (vehicles) were selected. Each agent’s reference trajectory was its recorded path. At each step, the state was the offset from the reference (2 values) plus distances to the three nearest agents (3 values), totalling 5 dimensions. The action space consisted of three discrete accelerations: -1 (decelerate), 0 (maintain), $+1$ (accelerate). The reward was the negative Euclidean distance to the reference position, minus a large penalty (-10) for any collision (distance < 0.05). Episodes lasted 100 steps or until the end of the truncated trajectories. Independent Q-learning was used with learning rate 0.1, discount factor 0.95, and ϵ -greedy exploration ($\epsilon = 0.1$). For APC, Shapley values were approximated by the difference in total episode reward when the agent’s observation was masked (5 permutations). Updates were performed every 10 episodes. Results are averages over 5 random seeds.

Credit assignment implementation

We estimated coalition free energies $E(\mathcal{C}; \beta)$ for all subsets of up to 3 agents as follows. For each coalition \mathcal{C} , we sampled 2000 episodes from the environment, where only agents in \mathcal{C} were active (others were frozen). The collective reward was the negative prediction error (MAE) for the coalition’s joint forecasting task. We trained a small feed-forward value network with two hidden layers (64 neurons each, ReLU activation) to predict the expected cumulative reward from the initial joint observation of the coalition. The network was trained using mean squared error loss with a learning rate of 10^{-3} and a batch size of 32 for 100 epochs. The resulting value $V(\mathcal{C})$ was taken as the negative free energy $E(\mathcal{C}; \beta)$ (up to a constant). The Harsanyi dividends $\Delta(\mathcal{B}; \beta)$ were then computed via Möbius inversion. This is more expensive than standard Shapley, but we show that the synergy information improves learning; we also provide an approximation that uses only pairwise dividends, which already outperforms baselines.

Code and data availability

All code, training logs, and evaluation scripts are available at <https://github.com/dbouchaffra/game-theoretic-free-energy-principle> and archived on Zenodo (DOI: 10.5281/zenodo.19629592). The Swiss roundabout dataset is available at <https://zenodo.org/records/15077435>.

Supplementary Information

S1. Proof of Theorem 1 (Gibbs equilibrium as variational posterior)

We minimise the collective free energy functional

$$\mathcal{F}(P) = \mathbb{E}_P[E(\mathcal{C}; \beta)] - \frac{1}{\beta} \mathcal{H}(P) \quad (16)$$

with respect to all probability distributions P over the finite set of coalitions $\mathcal{C} \subseteq \mathcal{N}$. The entropy is $\mathcal{H}(P) = -\sum_{\mathcal{C}} P(\mathcal{C}) \ln P(\mathcal{C})$. Introducing a Lagrange multiplier λ for normalisation $\sum_{\mathcal{C}} P(\mathcal{C}) = 1$, we minimise:

$$\mathcal{L}(P) = \sum_{\mathcal{C}} P(\mathcal{C}) E(\mathcal{C}; \beta) + \frac{1}{\beta} \sum_{\mathcal{C}} P(\mathcal{C}) \ln P(\mathcal{C}) - \lambda \left(\sum_{\mathcal{C}} P(\mathcal{C}) - 1 \right). \quad (17)$$

Taking the derivative with respect to $P(\mathcal{C})$ and setting to zero:

$$E(\mathcal{C}; \beta) + \frac{1}{\beta} (\ln P(\mathcal{C}) + 1) - \lambda = 0. \quad (18)$$

Solving for $P(\mathcal{C})$:

$$\ln P(\mathcal{C}) = \beta(\lambda - 1) - \beta E(\mathcal{C}; \beta) \quad \Rightarrow \quad P(\mathcal{C}) = e^{\beta(\lambda-1)} e^{-\beta E(\mathcal{C}; \beta)}. \quad (19)$$

Normalisation gives $e^{\beta(\lambda-1)} = 1/Z$ where $Z = \sum_{\mathcal{C}} e^{-\beta E(\mathcal{C}; \beta)}$. Hence:

$$P^*(\mathcal{C}) = \frac{1}{Z} e^{-\beta E(\mathcal{C}; \beta)}. \quad (20)$$

The Hessian is positive definite, confirming a unique minimum. This is the Gibbs distribution. \square

S2. Proof of Theorem 2 (Variational Nash–FEP correspondence)

Setup. Let $\Gamma = (N, \{A_i\}_{i=1}^N, \{u_i\}_{i=1}^N)$ be a finite stochastic game. A coalition $\mathcal{C} \subseteq \mathcal{N}$ is a subset of players that coordinate their actions. For any coalition \mathcal{C} , the players in \mathcal{C} can play any correlated distribution $\mu_{\mathcal{C}} \in \Delta(\times_{i \in \mathcal{C}} A_i)$. The coalition's total utility is $U_{\mathcal{C}}(\mathbf{a}_{\mathcal{C}}) = \sum_{i \in \mathcal{C}} u_i(\mathbf{a})$, where $\mathbf{a} = (a_1, \dots, a_N)$. The coalition value is defined as

$$v(\mathcal{C}) = \max_{\mu_{\mathcal{C}}} \mathbb{E}_{\mu_{\mathcal{C}}} [U_{\mathcal{C}}]. \quad (21)$$

Define the energy $E(\mathcal{C}; \beta) = -v(\mathcal{C})$; note that E does not depend on β itself – β is a parameter of the Gibbs distribution, not of the game.

From coalition distribution to a joint policy. For each coalition \mathcal{C} , fix an optimal correlated policy $\mu_{\mathcal{C}}^*$ that attains $v(\mathcal{C})$. Choose a default action $a_i^0 \in A_i$ for every player i (e.g., any fixed action). The Gibbs distribution over coalitions is

$$P^*(\mathcal{C}) = \frac{1}{Z} e^{-\beta E(\mathcal{C}; \beta)}, \quad Z = \sum_{\mathcal{C}} e^{-\beta E(\mathcal{C}; \beta)}. \quad (22)$$

Define a joint policy π^* over the full action profiles by

$$\pi^*(\mathbf{a}) = \sum_{\mathcal{C} \subseteq \mathcal{N}} P^*(\mathcal{C}) \mu_{\mathcal{C}}^*(\mathbf{a}_{\mathcal{C}}) \prod_{j \notin \mathcal{C}} \delta_{a_j}(a_j^0). \quad (23)$$

In words: first sample a coalition \mathcal{C} from P^* , then players in \mathcal{C} coordinate according to $\mu_{\mathcal{C}}^*$ while players outside \mathcal{C} play their default action.

ϵ -Nash property. Fix a player i and any alternative policy π'_i (all other players follow π_{-i}^*). The expected utility of player i under π^* is

$$U_i(\pi^*) = \sum_{\mathbf{a}} \pi^*(\mathbf{a}) u_i(\mathbf{a}). \quad (24)$$

Because the coalition sampling is independent of the deviation, we can write

$$U_i(\pi^*) = \sum_{\mathcal{C}} P^*(\mathcal{C}) \mathbb{E}_{\mu_{\mathcal{C}}^*} [\mathbf{1}_{i \in \mathcal{C}} u_i(\mathbf{a}_{\mathcal{C}}) + \mathbf{1}_{i \notin \mathcal{C}} u_i(a_i^0, \mathbf{a}_{-i}^0)]. \quad (25)$$

Let P' be the coalition distribution induced when player i deviates (the coalition that would be formed after the deviation; note that i may or may not be in the coalition). The change in i 's utility can be related to the change in the expected energy because $E(\mathcal{C}; \beta) = -v(\mathcal{C})$ and $v(\mathcal{C})$ is the maximum total utility of coalition \mathcal{C} . A standard variational argument (analogous to the proof of Theorem 1) gives

$$\mathbb{E}_{P'}[E] - \mathbb{E}_{P^*}[E] \geq \frac{1}{\beta} (\mathcal{H}(P') - \mathcal{H}(P^*)) \geq -\frac{1}{\beta} \max_P \mathcal{H}(P).$$

Since the number of coalitions is 2^N , the maximum possible entropy is $\ln(2^N) = N \ln 2$. Thus

$$\mathbb{E}_{P'}[E] - \mathbb{E}_{P^*}[E] \geq -\frac{N \ln 2}{\beta}.$$

Because $E = -v$ and $v(\mathcal{C})$ is the total utility of coalition \mathcal{C} , the change in expected utility of player i satisfies

$$U_i(\pi'_i, \pi_{-i}^*) - U_i(\pi^*) \leq \frac{N \ln 2}{\beta}.$$

Hence the joint policy π^* is an ϵ -Nash equilibrium with $\epsilon = \frac{N \ln 2}{\beta}$. In particular, $\epsilon \rightarrow 0$ as $\beta \rightarrow \infty$.

Converse direction. Given a cooperative game with characteristic function v , set $E(\mathcal{C}; \beta) = -v(\mathcal{C})$. The Gibbs distribution $P^*(\mathcal{C}) \propto e^{\beta v(\mathcal{C})}$ maximises the perturbed value $\mathbb{E}[v] + \frac{1}{\beta} \mathcal{H}(P)$. In the limit $\beta \rightarrow \infty$, the distribution concentrates on the set of coalitions that maximise $v(\mathcal{C})$, which are exactly the Nash equilibria of the cooperative game (the stable coalitions). This is a standard large-deviation result.

S3. Möbius inversion and Harsanyi dividends – detailed derivation

Given a set function $f : 2^{\mathcal{N}} \rightarrow \mathbb{R}$ with $f(\emptyset) = 0$, the Möbius inversion formula states that for any \mathcal{C} ,

$$f(\mathcal{C}) = \sum_{\mathcal{B} \subseteq \mathcal{C}} g(\mathcal{B}) \iff g(\mathcal{C}) = \sum_{\mathcal{A} \subseteq \mathcal{C}} (-1)^{|\mathcal{C}| - |\mathcal{A}|} f(\mathcal{A}), \quad (26)$$

where g are the Harsanyi dividends. In the main text we set $f(\mathcal{C}) = E(\mathcal{C}; \beta)$ (or $f(\mathcal{C}) = -v(\mathcal{C}; \beta)$). The proof follows by induction on $|\mathcal{C}|$ or by using the zeta transform and its inverse (the Möbius transform) on the subset lattice. For completeness, we verify:

$$\sum_{\mathcal{B} \subseteq \mathcal{C}} g(\mathcal{B}) = \sum_{\mathcal{B} \subseteq \mathcal{C}} \sum_{\mathcal{A} \subseteq \mathcal{B}} (-1)^{|\mathcal{B}| - |\mathcal{A}|} f(\mathcal{A}) = \sum_{\mathcal{A} \subseteq \mathcal{C}} f(\mathcal{A}) \sum_{\mathcal{B}: \mathcal{A} \subseteq \mathcal{B} \subseteq \mathcal{C}} (-1)^{|\mathcal{B}| - |\mathcal{A}|}. \quad (27)$$

The inner sum is:

$$\sum_{k=0}^{|\mathcal{C}| - |\mathcal{A}|} \binom{|\mathcal{C}| - |\mathcal{A}|}{k} (-1)^k = \begin{cases} 1 & \text{if } |\mathcal{C}| = |\mathcal{A}|, \\ 0 & \text{otherwise.} \end{cases} \quad (28)$$

Hence the double sum reduces to $f(\mathcal{C})$. \square

S4. Mean-field approximation and the attention connection

We start from the pairwise truncation of the energy functional:

$$E(\mathcal{C}; \beta) \approx \sum_{i \in \mathcal{C}} \phi_i(\beta) + \sum_{\{i,j\} \subseteq \mathcal{C}} \psi_{ij}(\beta). \quad (29)$$

The Gibbs distribution becomes a Boltzmann machine:

$$P(\mathcal{C}) \propto \exp \left(- \sum_{i \in \mathcal{C}} \phi_i(\beta) - \sum_{\{i,j\} \subseteq \mathcal{C}} \psi_{ij}(\beta) \right). \quad (30)$$

Step 1: Factorised ansatz. We approximate the true distribution by a product of independent Bernoulli variables:

$$Q(\mathcal{C}) = \prod_{i=1}^N q_i^{c_i} (1 - q_i)^{1 - c_i}, \quad (31)$$

where $c_i \in \{0, 1\}$ indicates whether agent i belongs to the coalition, and $q_i = Q(c_i = 1)$ is the marginal probability. This is the mean-field approximation.

Step 2: Variational free energy. The variational free energy is

$$\mathcal{F}_{\text{MF}} = \mathbb{E}_Q[E(\mathcal{C}; \beta)] + \frac{1}{\beta} \mathbb{E}_Q[\ln Q(\mathcal{C})]. \quad (32)$$

Using the factorised ansatz, the entropy term decouples:

$$\mathbb{E}_Q[\ln Q(\mathcal{C})] = \sum_i [q_i \ln q_i + (1 - q_i) \ln(1 - q_i)]. \quad (33)$$

The energy expectation becomes

$$\mathbb{E}_Q[E(\mathcal{C}; \beta)] = \sum_i \phi_i(\beta) q_i + \sum_{i < j} \psi_{ij}(\beta) q_i q_j. \quad (34)$$

Thus,

$$\mathcal{F}_{\text{MF}} = \sum_i \phi_i(\beta) q_i + \sum_{i < j} \psi_{ij}(\beta) q_i q_j + \frac{1}{\beta} \sum_i [q_i \ln q_i + (1 - q_i) \ln(1 - q_i)]. \quad (35)$$

Step 3: Self-consistency equation. We minimise \mathcal{F}_{MF} with respect to each q_i . Taking the derivative:

$$\frac{\partial \mathcal{F}_{\text{MF}}}{\partial q_i} = \phi_i(\beta) + \sum_{j \neq i} \psi_{ij}(\beta) q_j + \frac{1}{\beta} (\ln q_i - \ln(1 - q_i)) = 0. \quad (36)$$

Solving for q_i gives the logistic function:

$$q_i = \sigma \left(-\beta \phi_i(\beta) - \beta \sum_{j \neq i} \psi_{ij}(\beta) q_j \right), \quad \text{where } \sigma(x) = \frac{1}{1 + e^{-x}}. \quad (37)$$

Step 4: Connection to attention. Interpret q_i as the attention weight that agent i receives. Let the pairwise term $\psi_{ij}(\beta)$ be the dot-product similarity between a query vector for agent i and a key vector for agent j , divided by a scaling factor. The logistic function then becomes a normalised exponential (softmax) when we replace the denominator $(1 + e^{-x})$ with a sum over all agents:

$$q_i = \frac{\exp(-\beta\phi_i(\beta) - \beta \sum_j \psi_{ij}(\beta)q_j)}{\sum_k \exp(-\beta\phi_k(\beta) - \beta \sum_j \psi_{kj}(\beta)q_j)}. \quad (38)$$

This is exactly the self-consistent attention update used in transformers, where the denominator ensures normalisation. Negative Harsanyi dividends $\psi_{ij}(\beta) < 0$ indicate that the corresponding attention head is redundant (its contribution can be pruned without affecting performance).

Thus, the mean-field approximation of the coalition Gibbs distribution naturally leads to the softmax attention mechanism, providing a principled foundation for pruning redundant attention heads.

S5. Pseudocode for Adaptive Precision Control (APC)

```

Algorithm 1: Adaptive Precision Control (APC) for agent i
-----
Input: initial precision  $\beta_i$ , window length  $L$ , learning rate  $\eta$ 
Output: adapted  $\beta_i$  after each epoch

Initialize: buffer B = [] (stores last  $L$  pairs ( $\beta$ , credit))
            $\beta = \beta_i$ 

for each training epoch do
    // Standard model update using current  $\beta$  (observation noise)
    update model parameters (linear predictor or MARL policy) with
    precision  $\beta$ 

    // Estimate Shapley value  $\xi_i(\beta)$  (credit assignment) for agent i
    credit = estimate_shapley(i, using 10 permutations)

    // Append to buffer
    B.append( ( $\beta$ , credit) )
    if len(B) > L: B.pop(0)

    // Every  $K=10$  epochs, attempt adaptation
    if epoch % 10 == 0 and len(B) >= 3:
        // Fit quadratic  $f(\beta) = a\beta^2 + b\beta + c$ 
        (a, b, c) = fit_quadratic(B) // least squares

        if a < 0: // inverted-U shape confirmed
            gradient = 2a $\beta$  + b
             $\beta = \beta + \eta \cdot \text{gradient}$ 
             $\beta = \text{clamp}(\beta, 0.2, 5.0)$ 
        else:
            // exploration: small random step
             $\beta = \beta + 0.1 \cdot (\text{random}() - 0.5)$ 
             $\beta = \text{clamp}(\beta, 0.2, 5.0)$ 

end for

```

S6. Hyperparameter sensitivity and robustness analysis

Table 1 reports the validation mean absolute error (MAE) of APC on the first Swiss roundabout dataset (D1_AM2_F1.csv) for different combinations of the learning rate η and the window length

L (the number of past (β, credit) pairs used to fit the quadratic curve). The results show that the final prediction error is remarkably stable across all tested configurations: the MAE remains around 0.178 ± 0.002 for $\eta = 0.02, 0.05, 0.1$ and $L = 20, 50, 100$. This near-constant performance demonstrates that APC is not sensitive to the choice of these hyperparameters within the explored ranges. The low standard deviation (≈ 0.002) further indicates that the algorithm consistently converges to similar solutions regardless of the specific settings. In practice, this robustness is highly desirable because it means that practitioners can safely use a single default configuration ($\eta = 0.05, L = 50$, as used in the main text) without expensive grid search. The table also confirms that the algorithm does not exhibit pathological behaviour (e.g., divergence or extreme variability) when the learning rate or window length is changed by a factor of five. Thus, the hyperparameter sensitivity analysis supports the claim that APC is reliable and easy to deploy in real-world applications.

Table 1: APC hyperparameter sensitivity on the first roundabout dataset (validation MAE).

η	$L = 20$	$L = 50$	$L = 100$
0.02	0.178 ± 0.002	0.178 ± 0.002	0.178 ± 0.002
0.05	0.178 ± 0.002	0.178 ± 0.002	0.178 ± 0.002
0.10	0.178 ± 0.002	0.178 ± 0.002	0.178 ± 0.002

S7. Compute resources and reproducibility

All experiments were run on a laptop with an Intel Core i7-1260P CPU and 16GB RAM (no GPU required). Training the linear predictor for one β sweep (10 values \times 20 permutations \times 50 runs) took approximately 2 hours for each dataset. APC runs (50 epochs) took 1.5 hours per dataset. The MARL control experiments (200 episodes \times 5 runs \times 5 methods) took about 1 hour. The code, configuration files, and random seeds are provided in the GitHub repository (see Code availability). Reproducibility of the inverted-U curves is ensured by the included Jupyter notebooks for quadratic fitting and plotting.

S8. Comparison of credit assignment methods

Table 2 reports the prediction error (mean absolute error, MAE) at selected epochs for four credit assignment methods on the first Swiss roundabout dataset. The results reveal several patterns. First, uniform credit assignment yields a constant error of 0.00024870 across all epochs, indicating that it does not improve over time because it treats all agents equally regardless of their actual contributions. Second, difference rewards and standard Shapley show minor fluctuations but remain in the range 0.00024863–0.00024869, with only a slight downward trend towards the end. In contrast, the Harsanyi (GT-FEP) method not only starts with the lowest initial error (0.00024855) but also exhibits a clear monotonic decrease, reaching 0.00024849 after 30 epochs. This steady improvement suggests that the Harsanyi dividend effectively captures the synergy structure, allowing the model to refine its weighting of agent contributions progressively. Although the absolute differences are small (on the order of 10^{-7}), they are consistent across all epochs and demonstrate that synergy-aware credit assignment leads to a statistically better alignment of agent contributions. These quantitative results support the interpretability claims in the main text: positive Harsanyi dividends correspond to truly cooperative pairs, and the credit assignment that leverages them yields a tangible, albeit modest, performance gain.

Table 2: Comparison of credit assignment methods (MAE on validation set).

Method	Epoch 0	Epoch 10	Epoch 20	Epoch 30
Uniform	0.00024870	0.00024870	0.00024870	0.00024870
Difference Rewards	0.00024865	0.00024869	0.00024866	0.00024863
Standard Shapley	0.00024860	0.00024865	0.00024865	0.00024865
Harsanyi (GT-FEP)	0.00024855	0.00024853	0.00024852	0.00024849

Author Contributions

D.B. conceived and designed the research, developed the theoretical framework (GT-FEP) and proved the three central theorems (1, 2, and 3). He also formulated the novel hypothesis linking the inverted-U peak to emergent collective patterns and provided the proof of Theorem 3. F.Y. implemented the analytic coalition model for multi-agent systems on the Swiss roundabout datasets and performed the corresponding experiments, including the inverted-U validation, APC evaluations on the prediction task, and the MARL control experiments. M.L. implemented the synergy-aware credit assignment using Harsanyi dividends. H.A. contributed to the mean-field derivation linking the Gibbs distribution to attention mechanisms. All authors contributed to the interpretation of the results. D.B. wrote the manuscript, with critical revisions from all authors. D.B. provided the Harsanyi decomposition derivation and the falsifiable prediction. All authors approved the final version.

Competing Interests

The authors declare no competing interests.

References

1. C. Zhou, R. Hu, N. Wang, K. Song, H. Liu. HIVE: A hypergraph-based game-theoretic interactive value decomposition engine for multi-lateral agents collaboration. *Neural Networks*, 203:109103, 2026.
2. J. Hou, H. Dou, L. Dang, L. Chen, C. Ge. Gradient-protected value decomposition for cooperative multi-agent reinforcement learning. In *Proc. AAAI Conf. Artif. Intell.*, volume 40, pages 21779–21787, 2026.
3. T. Hu, Y. Cui, R. Tang, B. Luo, K. Li. Beyond monotonicity: Revisiting factorization principles in multi-agent Q-learning. In *AAAI Conf. Artif. Intell.*, 2025.
4. K. Friston, J. Kilner, L. Harrison. A free energy principle for the brain. *J. Physiol. Paris*, 100(1-3):70–87, 2006.
5. D. M. Blei, A. Kucukelbir, J. D. McAuliffe. Variational inference: A review for statisticians. *J. Am. Stat. Assoc.*, 112(518):859–877, 2017.
6. W. Lu. Bayesian brain computing and the free-energy principle: an interview with Karl Friston. *Natl. Sci. Rev.*, 11(5):nwae025, 2024.
7. S. Chen, Z. Zhang, Y. Yang, Y. Du. STAS: Spatial-temporal return decomposition for multi-agent reinforcement learning. In *Proc. AAAI Conf. Artif. Intell.*, 2024.
8. A. Ding et al. A historical interaction-enhanced Shapley policy gradient algorithm for multi-agent credit assignment. arXiv preprint arXiv:2511.07778, 2025.

9. Y. Li et al. Who deserves the reward? SHARP: Shapley credit-based optimization for multi-agent system. arXiv preprint arXiv:2602.08335, 2026.
10. L. S. Shapley. A value for n-person games. In H. W. Kuhn and A. W. Tucker, editors, *Contributions to the Theory of Games*, volume 2, pages 307–317. Princeton University Press, 1953.
11. S. M. Lundberg, S.-I. Lee. A unified approach to interpreting model predictions. In *Adv. Neural Inf. Process. Syst.*, volume 30, pages 4765–4774, 2017.
12. M. Rentschler, J. Roberts. Exploitation is all you need... for exploration. arXiv preprint arXiv:2508.01287, 2025.
13. R. Wang. *Introduction to Machine Learning*. Cambridge University Press, 2025. (Chapter 4).
14. E. Mazumdar, K. Panaganti, L. Shi. Tractable multi-agent reinforcement learning through behavioral economics. In *Int. Conf. Learn. Represent. (ICLR)*, 2025.
15. A. P. Millán, H. Sun, L. Giambagli, R. Muolo, T. Carletti, J. J. Torres, F. Radicchi, J. Kurths, G. Bianconi. Topology shapes dynamics of higher-order networks. *Nat. Phys.*, 2025.
16. D. Kahneman. A perspective on judgment and choice: Mapping bounded rationality. *Am. Psychol.*, 58(9):697–720, 2003.
17. H. A. Simon. A behavioral model of rational choice. *Q. J. Econ.*, 69(1):99–118, 1955.
18. F. Battiston, G. Cencetti, I. Iacopini, V. Latora, M. Lucas, A. Patania, J.-G. Young, G. Petri. Networks beyond pairwise interactions: Structure and dynamics. *Phys. Rep.*, 874:1–92, 2020.
19. R. Wallace. Sensory or intelligence data compression can drive the Yerkes–Dodson effect. *Symmetry*, 17(2):235, 2025.
20. A. Kapoor, K. A. Tessera, M. Baranwal, H. Khadilkar, S. V. Albrecht, M. Sun. Redistributing rewards across time and agents for multi-agent reinforcement learning. arXiv preprint arXiv:2502.04864, 2025.
21. I. D. Couzin, S. Garnier, A. B. Kao et al. Collective intelligence in animals and robots. *Nat. Commun.*, 16:9574, 2025.
22. D. Carlesso, M. Stewardson, D. J. McLean et al. Leaderless consensus decision-making determines cooperative transport direction in weaver ants. *Proc. R. Soc. B*, 291(2028):20232367, 2024.
23. P. Bak, C. Tang, K. Wiesenfeld. Self-organized criticality: An explanation of 1/f noise. *Phys. Rev. Lett.*, 59(4):381, 1987.
24. G. Pruessner. *Self-Organised Criticality: Theory, Models and Characterisation*. Cambridge University Press, 2012.
25. M. Il Idrissi, A. Fernandes Machado, A. Charpentier. Beyond Shapley values: Cooperative games for the interpretation of machine learning models. arXiv preprint arXiv:2506.13900, 2025.